Coherent Photonic Processing of Microwave Signals Using Spatial Light Modulators: Programmable Amplitude Filters

Shijun Xiao, *Member, IEEE*, and Andrew M. Weiner, *Fellow, IEEE*

***Abstract*—This paper presents a novel coherent optical signal processing approach for synthesis of programmable microwave amplitude filters over an ultrawideband. The authors' scheme relies on a programmable hyperfine optical filter implemented in a pulse-shaping geometry, which provides arbitrary, user-defined amplitude-filtering functions over a 50-GHz bandwidth with resolution better than 0.7 GHz. In contrast to previous work on discrete time optical processing of microwave signals, their approach allows direct synthesis of microwave filter functions in spectral domain without computing filter coefficients, which is needed for a discrete-time-domain approach.**

***Index Terms*—Microwave photonics, optical filters, optical signal processing, pulse shaping.**

I. Introduction

PHOTONIC processing of microwave signals has been explored for nearly 30 years [1]–[4]. In general, microwave signals are imposed onto an optical carrier, manipulated directly in the optical domain, and then converted back into the microwave domain through optical-to-electrical (O/E) receivers [photodiodes (PDs)]. Compared to conventional electronic processing, advantages of photonic processing include ultrawide bandwidth, immunity to electromagnetic interference, flexibility, etc., which bring attractive applications prospects in microwave and millimeter wave engineering [5], [6]. Previous approaches have been referred to as discrete-time optical processing of microwave signals (DOPMSs) [1], which can be modeled as tapped nonrecursive (finite impulse response) or recursive (infinite impulse response) digital filters. Generally, DOPMS can be classified into two operation regimes: coherent processing based on addition of fields, with laser coherence time $(\tau_c) \gg$ tap delay (T), and incoherent processing $(\tau_c \ll T)$ based on addition of powers. Since coherent DOPMS is very sensitive to environmental conditions [4], incoherent DOPMS has been widely applied. Two main schemes to implement delay lines for incoherent DOPMS are classical fiber delay-line filters and fiber grating delay-line filters [7], [8]. Incoherent DOPMS in its early incarnations provided only positive filter coefficients, which limits the ability to achieve flat filtering bands and sharp transitions. Consequently, much recent effort has been focused on realization of incoherent DOPMS architectures providing negative filter coefficients. Recent results may be found in references [9]–[14]. Another important direction in incoherent DOPMS research aims at realization of filters with large numbers of taps, particularly in configurations compatible with flexible reprogramming. Furthermore, most experimental realizations of incoherent DOPMS provide free spectral ranges (FSRs) $(\text{FSR} \sim 1/T)$ of only several gigahertz. This is not a fundamental limitation of DOPMS but is subject to the practical requirement to implement small tap delays with sufficient precision. A fixed eighteen-tap filter with 10-GHz FSR implemented using advanced fiber-Bragg-grating-fabrication methods was reported in [15]. Large FSRs of at least 10 GHz will be useful for applications such as ultrawideband (UWB) wireless [16]. In addition to research on incoherent DOPMS, some work on filters based on coherent optical processing using tapped waveguide delay-line structures has been reported [17], but further development is needed.

In this paper, we introduce a novel coherent processing scheme based on an optical parallel filtering in the frequency domain in conjunction with optical heterodyning, rather than the traditional tapped delay-line approach. As a result, we are able to demonstrate filters with nearly flat-topped passband response and with sharp transitions that can be placed anywhere within a microwave band up to 20 GHz (higher operating bandwidths are possible). We also demonstrate a full programmability that allows realization of reconfigurable and essentially arbitrary microwave amplitude filters over the 20-GHz band. The frequency domain optical filtering is implemented using programmable pulse-shaping techniques [18], that are for the first time extended to hyperfine ($\sim$ 500 MHz) spectral resolution through the use of a virtually imaged phased array (VIPA) spectral disperser [19]. Our spectral domain pulse-shaping architecture provides a fully coherent optical processing without significant sensitivity to environment conditions. The resultant microwave filter allows essentially arbitrary amplitude filtering over a microwave band from below 1 to 20 GHz with 500-MHz resolution under a programmable control. Comparable capability has not been previously reported, to the best of our knowledge.

The remainder of this paper is structured as follows. A theoretical analysis is presented in Section II. Section III introduces the experimental setup. Section IV discusses our experimental results on optical amplitude filtering. Section V discusses our

Manuscript received September 27, 2005; revised November 11, 2005. This work was supported in part by DARPA under the SPAWAR Systems Center, San Diego, under Contract N6601-06-1-2006. Any opinions, findings, and conclusions or recommendations expressed in this publication are those of the authors and do not necessarily reflect the views of DARPA and SPAWAR.

The authors are with the School of Electrical and Computer Engineering, Purdue University, West Lafayette, IN 47907-2035, USA (e-mail: sxiao@ecn.purdue.edu; amw@ecn.purdue.edu).

Digital Object Identifier 10.1109/JLT.2006.874649

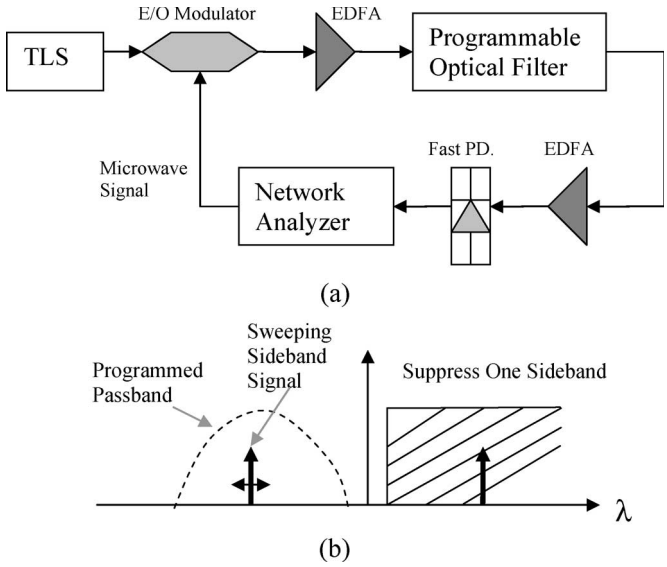

Fig. 1. (a) Experimental setup for photonic processing of microwave signals. Tunable laser source (TLS) and erbium doped fiber amplifier (EDFA). (b) Optical spectral sketch to illustrate the general principle of photonic processing.

experimental results on microwave amplitude filtering. We conclude in Section VI.

II. Theoretical Discussions

Fig. 1 shows our setup to implement coherent photonic processing of microwave signals via programmable hyperfine optical spectral filtering. A continuous wavelength (CW) optical carrier is passed through a Mach–Zehnder intensity modulator (MZM) driven by the microwave input signal. Here, we consider the case of input microwave signals that are single-frequency tones. This is appropriate for comparison to the swept-frequency measurements used in experiments. The modulator output field has a double-sideband format. Optical filtering suppresses one sideband while passing the carrier and the other sideband. The amplitude of the remaining sideband is manipulated by the programmable hyperfine optical filter. The result is converted back to a microwave signal by heterodyne beating with the carrier on a fast PD.

If we assume that the microwave tone signal is applied to a single arm of the Mach–Zehnder modulator, the output optical field $E(t)$ can be described by

$$E(t) \propto \mathrm{Re}\left\{e^{j\omega_c t} + e^{j[\omega_c t+\delta+\pi A\cos(\Omega t)/V_\pi]}\right\} \quad (1)$$

where $\mathrm{Re}\{\}$ indicates the real part, ω_c is the optical carrier frequency, $\delta = \pi V_b/V_\pi$ is the phase shift caused by the dc bias V_b, V_π is the minimum transmission voltage parameter of the modulator, and $A\cos(\Omega t)$ is the input microwave tone signal.

The Taylor series expansion in $\pi A/V_\pi$ is

$$E(t) \propto \mathrm{Re}\left\{e^{j\omega_c t} + e^{j(\omega_c t+\delta)}\left[1 + j\frac{\pi A}{V_\pi}\cos(\Omega t) - \frac{1}{2}\left(\frac{\pi A}{V_\pi}\right)^2\cos^2(\Omega t) + \ldots\right]\right\} \quad (2)$$

where $\pi A/V_\pi < 1$ is required to make sure the series expansion converges.

For a small signal modulation ($\pi A/V_\pi \lesssim 0.1$), we focus on linear modulation (ignoring the second or higher order terms in the expansion). The first order approximation of $E(t)$ is

$$E(t) \propto \mathrm{Re}\left\{e^{j\omega_c t} + e^{j(\omega_c t+\delta)}\left[1 + j\frac{\pi A}{V_\pi}\cos(\Omega t)\right]\right\} \quad (3)$$

which is equivalent to

$$E(t) \propto \mathrm{Re}\left\{\left[e^{j\omega_c t} + e^{j(\omega_c t+\delta)}\right] + j\frac{\pi A}{2V_\pi}e^{j(\omega_c t+\Omega t+\delta)} + j\frac{\pi A}{2V_\pi}e^{j(\omega_c t-\Omega t+\delta)}\right\}. \quad (4)$$

Now, we assume that an optical filter suppresses one sideband while modifying the amplitude of the remaining sideband. The result is

$$E(t) \propto \mathrm{Re}\left\{\left[e^{j\omega_c t} + e^{j(\omega_c t+\delta)}\right] + j\gamma(\omega_c+\Omega)\frac{\pi A}{2V_\pi}e^{j(\omega_c t+\Omega t+\delta)}\right\} \quad (5)$$

where $\gamma(\omega_c+\Omega)$ represents the frequency dependent amplitude transmission coefficient. Although in general, the frequency dependent transmission coefficient of the optical filter can be complex, here we specialize to amplitude filtering (γ is real, $0 \le \gamma(\omega_c+\Omega) \le 1$). Phase filtering will be considered elsewhere. In our treatment, we assume that the higher frequency (shorter wavelength) sideband is chosen. Note however that in general either one of the two sidebands can be chosen.

The PD current output is

$$i(t) \propto I(t) \propto \left\langle E^2(t)\right\rangle_{\omega_c} \propto 2\cos^2(\delta/2) + \frac{1}{2}\left[\gamma_m(\Omega)\frac{\pi A}{2V_\pi}\right]^2 - \cos(\delta/2)\gamma_m(\Omega)\frac{\pi A}{V_\pi}\sin(\Omega t+\delta/2) \quad (6)$$

where $i(t)$ is the PD current and $I(t)$ is the optical intensity averaged over the oscillations of the optical carrier. Please note that we assume a linear PD: The current is proportional to the input light intensity. For simplicity, we have introduced the notation $\gamma_m(\Omega) = \gamma(\omega_c+\Omega)$. The voltage signal consists of a dc component as well as a filtered ac signal. For the ac signal, (6) represents an amplitude filter with spectral response $\gamma_m(\Omega)$.

According to expression (6), a sufficient condition to have a nonzero signal $u(t)$ is that $\cos(\delta/2)$ is not equal to zero, and this requires $\delta = \pi V_b/V_\pi$ not to be odd multiples of π. In fact, this condition means that we must maintain a certain optical carrier at the modulator output, which is required for heterodyne beating. A large magnitude of optical sideband is favorable to obtain a large microwave signal, but it is limited by the condition for modulation linearity, i.e., $\pi A/V_\pi \lesssim 0.1$. According to (6), biasing the modulator for a large magnitude of optical carrier is also favorable to obtain a large microwave signal. However, this changes in the case of a saturated optical amplifier

(as in our experiments). For a strongly saturated amplifier, one can show that in order to maximize the ac signal in (6), the carrier and the sideband should have approximately equal power in the link, i.e., $|\cos(\delta/2)| \approx \pi A/V_\pi$. Our experiments are adjusted to satisfy this condition. Thus, for simplicity we ignore gain in above discussion.

III. Experimental Setup

Our experiments on photonic-assisted microwave filtering use a tunable laser with linewidth below 0.1 pm ($\sim$ 12.5 MHz) as the optical carrier. A MZM with an electrical -3 dB passband $>$ 30 GHz is used to modulate the microwave signal onto the optical carrier. The modulator has a single electrode input and a minimum transmission voltage $V_\pi \sim 5.0$ V. The input microwave tone from a network analyzer is swept from 0.05 to 20.05 GHz (instrumental limit) at a step of 0.05 GHz with a constant RF power level at -5 dBm corresponding to an amplitude voltage of 0.18 V for 50-Ω impedance ($\pi A/V_\pi = 0.11$). The modulator is biased for double-sideband modulation with partial carrier suppression, where the carrier is maintained at approximately the same power level as the modulation sidebands. After being amplified by an erbium-doped fiber amplifier (EDFA) to a total power $\sim$ 5 dBm, the signal passes through the programmable optical filter (discussed in the following). The output is a single-sideband signal with carrier, with one sideband suppressed by the optical filter by $>$ 25 dB (for sideband frequencies $> \sim$ 0.6 GHz, discussed in filtering results). Simultaneously, the remaining single sideband is also processed by the optical filter; this is a key concept for out photonic filtering scheme. A second EDFA is used to amplify the input optical power into the fast PD, which has an electrical -3-dB bandwidth of $\sim$ 60 GHz. The microwave signal is recovered by heterodyne beating via the fast PD. Finally, the output microwave signal is measured by the network analyzer.

Fig. 2 shows the setup of our programmable optical filter. The filter is implemented using a reflective geometry pulse shaper, where a VIPA rather than a grating is used as the optical spectral disperser. The VIPA has a FSR of 50 GHz (0.4 nm) at 1.55 μm. It can provide a large angular dispersion $\geq 3^\circ$/nm as well as an ultranarrow bandwidth when used as a demultiplexing filter (-3-dB bandwidth of $\sim$ 0.7 GHz at 1.55 μm). We previously demonstrated this narrow linewidth feature in implementing a fixed hyperfine wavelength demultiplexer with channel spacing of $\sim$ 3 GHz [20]. The VIPA has also been used in a pulse-shaping geometry with mechanically tuned slits as a blocking filter with a narrow skirt of $\sim$ 1000 dB/nm, which we have exploited in optical single-sideband-modulation experiments [21]. Using these VIPA-based filters, we have also previously demonstrated a novel multiple-channel hybrid subcarrier multiplexing (SCM)-WDM fiber communication system [22], where very narrow WDM channel spacings of $\sim$ 3 GHz were achieved. Another group has used a VIPA in a reflection pulse shaper together with fixed phase masks, in order to demonstrate optical code-division multiple-access phase encoding with 5-GHz frequency resolution [23]. Our group has recently achieved the first implementation of an electronically programmable VIPA-based pulse shaper incorporating a liquid-crystal spatial light modulator (SLM) [24], which we configured for spectral phase control. In that work, using a 400-GHz FSR VIPA, the spectral resolution was on the order of a few tens of gigahertz. In the current paper, we demonstrate the first VIPA-based pulse shaper using an SLM for programmable spectral amplitude control. Compared to [24], we now achieve a substantially better spectral resolution of 500–700 MHz, which is a key enabler for the programmable microwave-filtering application.

In our implementation of Fig. 2, the input is linearly polarized in x and incident into the VIPA with $\sim 2.5^\circ$ incident angle. The input optical frequency components are dispersed by the VIPA and collimated by a cylindrical lens (CYL) with a focal length of 300 mm. A standard programmable SLM is placed at the back focal plane of the focusing lens. The liquid-crystal SLM comprises 128 pixels, with pixel-to-pixel spacing of 100 μm. A flat mirror very close to the SLM reflects the light that then double passes through the SLM. Theoretically, a dispersion-free setup can be achieved with proper VIPA-lens separation. For amplitude modulation, we insert a polarizer, e.g., an x-polarizer (not shown in Fig. 2), between the collimator and the CYL preceding the VIPA. With appropriate programming, the SLM rotates a linearly x-polarized input to a linearly y-polarized output after a double pass, so an OFF state results when the return light passes through the polarizer. States between ON and OFF can also be generated (gray-level amplitude attenuation) as desired by programming the SLM. Reprogramming speed is dictated by the SLM response, which is on the order of tens of milliseconds scalable down to perhaps milliseconds for the liquid crystal displays commonly used in pulse shaping [18].

IV. Optical Amplitude Filtering

Before characterizing the microwave-filtering response of our entire system, we first report measurements of the programmable optical filter. As described in the previous section, our setup is the first fully programmable hyperfine optical filter using an SLM in a VIPA-based pulse shaper.

First, a blocking filtering is needed to generate a single-sideband signal from the original double-sideband format by suppressing one of the sidebands. In our scheme, we use a single VIPA-based pulse-shaper setup both to suppress one sideband and to control the amplitude of the retained sideband. In this scheme, half of the VIPA filter's FSR is needed for sideband suppression, and this leaves half of the FSR available for programmable filtering. The measurements here are taken by sweeping the tunable laser source with a step of 1 pm (125 MHz). Fig. 3(a) shows the optical power transmission by turning on pixels #40–#75. The result is an optical bandpass filter with $\sim$ 25-GHz bandwidth and sharp edges. The optical carrier wavelength is located around 1550 nm, corresponding to pixel #75 of the SLM. In fact, as the network analyzer used in our measurements works only up to 20 GHz, only pixels #45–#75 corresponding to $\sim$ 20-GHz bandwidth are used. The contrast ratio (between the passband and the background) is $>$ 25 dB, which is also the maximum sideband suppression

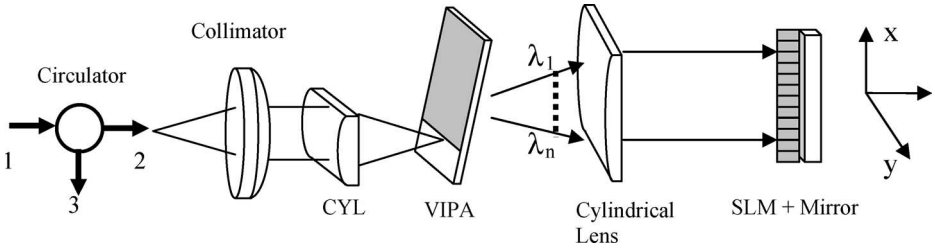

Fig. 2. Experimental setup of our programmable coherent optical filter based on a virtually imaged phased-array: cylindrical lenses (CYL) and spatial light modulator (SLM).

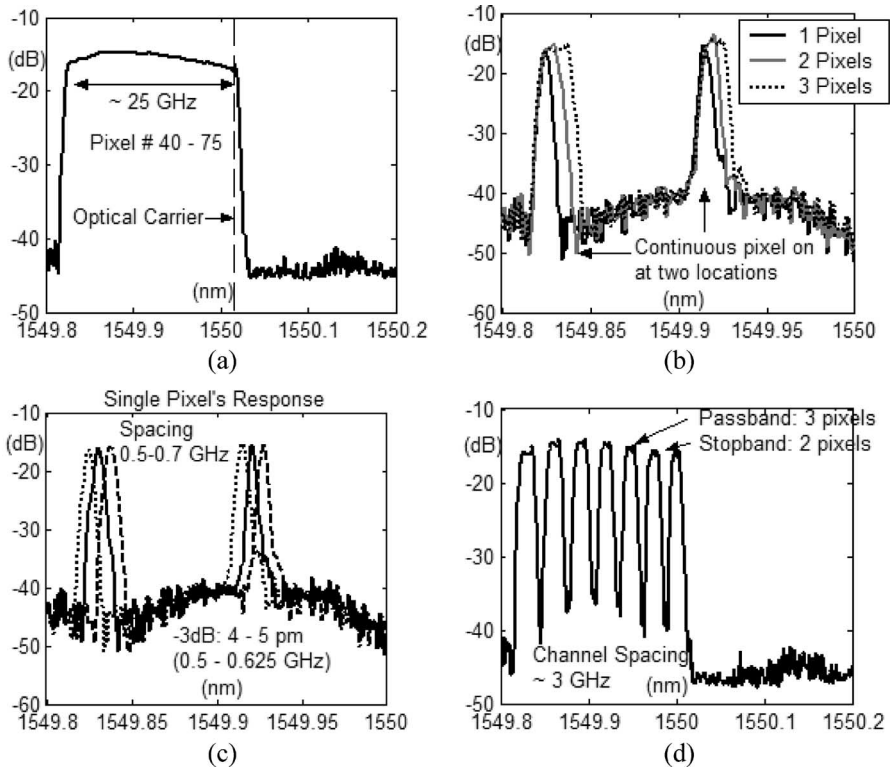

Fig. 3. Characterizations of programmable optical filters based on a virtually imaged phased-array. (a) Transmission response with pixel #40–#75 turned on, (b) single pixel response versus double or triple continuous adjacent pixels' response, (c) single pixel response at three continuous adjacent pixels, respectively, and (d) an example of optical comb filtering.

ratio. The remaining background level is mainly attributed to nonideal reflections in the filter after circulator port 2, such as a slight reflection from the input face of the VIPA. The total fiber-to-fiber insertion loss is $\sim$ 15 dB (including $\sim$ 2 dB circulator loss) but may be reduced to $\sim$ 8 dB in theory. Although not shown in the figures, the transmission repeats periodically with period of $\sim$ 50 GHz ($\sim$ 0.4 nm). Fig. 3(b) and (c) shows an optical power transmission spectra for examples where only a few pixels are turned on; this is used to measure the spectral resolution of the optical filter. In Fig. 3(b), passbands consisting of one, two, or three pixels are turned on at two separate wavelengths. The transmission with only one pixel reaches approximately the same level as that with two or three adjacent pixels turned on. This indicates that each pixel is resolved and can independently control a small band of wavelength components. In Fig. 3(c), the filter is programmed for two separated passbands, where each is one-pixel wide. The three different curves are similar except for shifts of -1, 0, or 1 pixel, respectively. The pixel-to-pixel spacing is 0.5–0.7 GHz, and the -3-dB bandwidth of a one-pixel-wide passband filter is 0.5–0.625 GHz. The average angular dispersion is $\sim 4^\circ/\text{nm}$ corresponding to an average pixel-to-pixel channel spacing of $\sim$ 0.6 GHz. These optical filter properties will limit the finest resolution that can be attained in microwave filtering to 500 MHz since there is a direct mapping from optical to microwave filtering. Fig. 3(d) is an example that illustrates the general programmability of our optical filters. Here, the filter consists of multiple flat-topped passbands (three pixels each) separated by sharp notches (two pixels each). The channel spacings are obviously nonuniform, which is expected, given nonlinearity in the VIPA's spectral dispersion law, which has been studied in our previous work [25].

V. Microwave Amplitude Filtering

The programmable optical filtering capabilities demonstrated in Section IV can be directly mapped to the microwave domain via heterodyne conversion. The results in a microwave filter

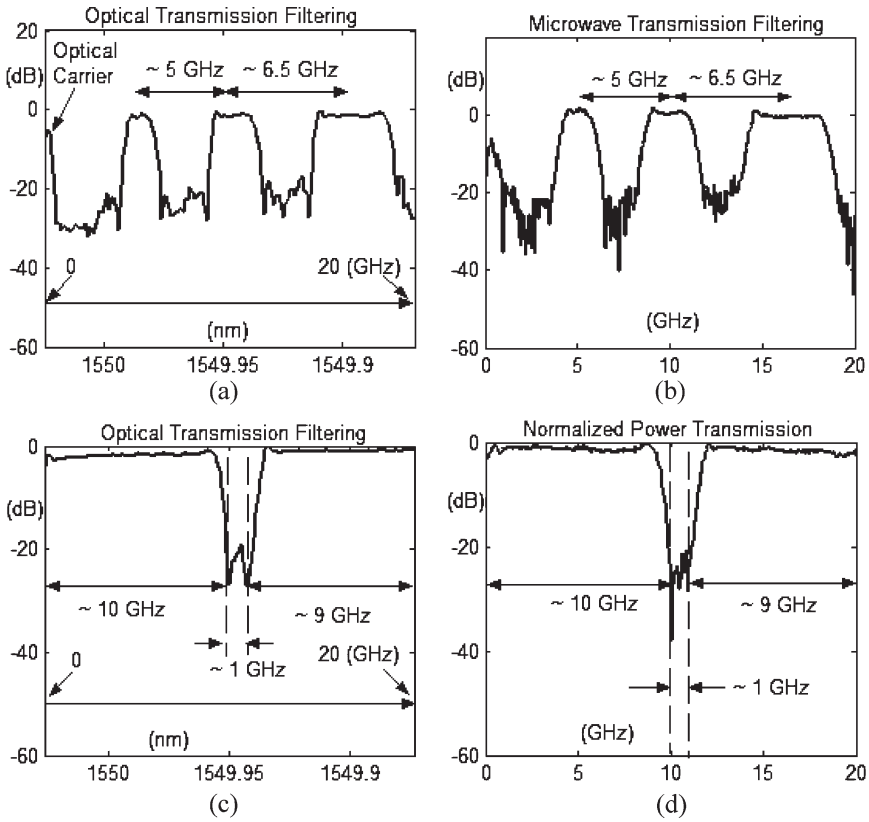

Fig. 4. Correspondence between optical filtering and microwave filtering. (a) Optical multipassband filtering, (b) corresponding microwave multipassband filtering, (c) optical notched filtering, and (d) corresponding microwave notched filtering.

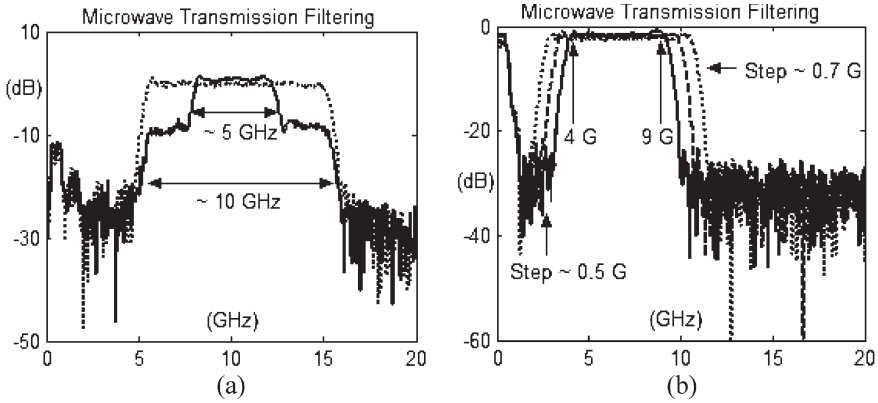

Fig. 5. Engineerable microwave filtering. (a) Microwave bandpass filtering with stepped response and (b) microwave bandpass filtering compatible to UWB spectral range 3.1–10.6 GHz.

functionality that can be measured through the network analyzer. Fig. 4 shows two examples of the mapping from optical filter to microwave filter. The power transmission responses are plotted over a 20-GHz band. (The power transmission is normalized for comparisons; the minimum microwave insertion loss is $\sim$ 8 dB for the filters implemented in our current setup). Fig. 4(a) shows an optical filter with multiple flat-topped passbands, different passband widths and spacings, and sharp transitions. Fig. 4(b) shows the corresponding microwave filter response after the heterodyne conversion. The similarity is very clear. Fig. 4(c) is an example of a band stop or notch optical filter, and Fig. 4(d) is the corresponding microwave filter response after the heterodyne conversion. Both exhibit a similar notch with a bandwidth $\sim$ 1 GHz. Two additional examples of programmable-engineered microwave filters are shown in Fig. 5. The transmission is also normalized. Fig. 5(a) is an example of stepped bandpass microwave filtering with a flat-topped response, where the step depth can be easily controlled by programming. Starting with a filter with a flat $\sim$ 10-GHz passband as a reference (dotted curve), we program in two steps that drop down by $\sim$ 10 dB symmetrically within the passband. With our programmable approach to photonic filtering, microwave-filtering functions can be easily engineered for specific applications. Fig. 5(b) is an example

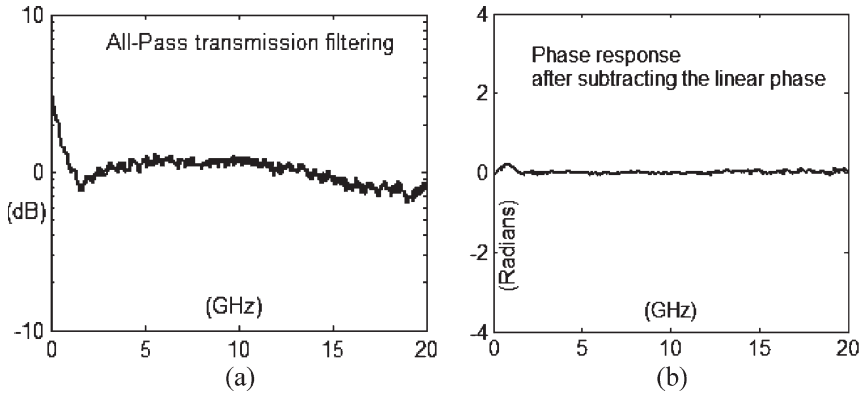

Fig. 6. Phase response of programmed microwave filters. (a) All-pass power transmission without amplitude modulation and (b) corresponding phase response for all-pass filtering.

of amplitude passband filtering that approximately conforms to the 3.1–10.6 GHz UWB band defined by the Federal Communications Commission (FCC) [16]. The edges of the passband can be tuned at a minimum step of 0.5–0.7 GHz corresponding to the adjacent pixel spacing discussed in Section IV.

It is interesting to briefly discuss the phase response of our photonically implemented microwave filters. As is evident from (6), the microwave and optical phase response are directly linked. Since optical pulse shapers can be set up to be dispersion free [18], we expect the microwave response to exhibit linear phase. Fig. 6(a) shows the microwave amplitude response when the SLM is programmed for full transmission; the response is nearly flat, similar to the optical intensity response in Fig. 3(a). Fig. 6(b) shows the corresponding microwave phase response, with the linear phase subtracted for clarity of illustration. As expected, the phase is nearly flat over a full 20-GHz range. Similar results are obtained for the structured microwave filters of Figs. 4 and 5: Close to flat phase is observed within the passbands of all the filters investigated.

One point to be pointed out is that a low pass transmission always exists below 600 MHz or so in Figs. 4(b) and 5. This residual low pass response is mainly the passband of a single pixel that must be turned on to pass the carrier (required for heterodyne beating). Although the lowpass transmission may be partially suppressed via some fine tunings in our experiments, i.e., Figs. 4(b) and 5(a), a different scheme is needed to cancel it fundamentally. One approach is simply to use an electrical dc blocking filter.

In addition to flexible implementations of various microwave-filter-response functions as we have discussed, the gain of the filter is another important parameter in practical applications. One important merit of photonic-assisted filtering is that wideband optical amplification (EDFA) can be used in the photonic loop to improve the microwave gain, subject of course to additional noise resulting from the amplification process. Progress in optical devices optimized generally for microwave photonics applications can also be exploited to enhance our coherent photonic microwave-filtering scheme. For example, modulators with high linearity as well as low driving voltage are desirable, as are PDs with high responsitivity and high-current handling capabilities. By employing state-of-the-art microwave photonic devices, our approach should be able to provide coherent photonic processing of microwave signals, both with great flexibility and easy reconfigurability and with high efficiency.

VI. Conclusion

We have demonstrated a novel scheme for photonic processing of microwave signals, which is fundamentally different from previous approaches (DOPMS) pursued over more than two decades. Our approach is based on a programmable hyperfine optical spectral filter, which uses a SLM within a reflective Fourier transform pulse-shaper geometry to provide arbitrary user-defined filtering functions over a 50-GHz optical band with resolution better than 0.7 GHz. Heterodyne conversion yields a microwave output, where the optical filter function is directly downshifted to microwave frequencies. In contrast to previous work, our approach uses the optical signals in a fully coherent way and implements filters directly in the spectral domain rather than the traditional discrete time domain. We have presented several examples demonstrating microwave-filtering functions over a 20-GHz band. Our results include filters with flat-topped and nonperiodic spectral responses and with low-side lobes over the full 20-GHz band.

Acknowledgment

The authors would like to thank C. Lin from Avanex Corporation for providing VIPA devices. The authors would also like to thank both Prof. D. Peroulis and Prof. W. J. Chappell from Purdue University for loaning the network analyzer.

References

[1] J. Capmany, B. Ortega, D. Pastor, and S. Sales, "Discrete-time optical processing of microwave signals," *J. Lightw. Technol.*, vol. 23, no. 2, pp. 702–723, Feb. 2005.

[2] C. Chang, J. A. Cassaboom, and H. F. Taylor, "Fiber optical delay line devices for RF signal processing," *Electron. Lett.*, vol. 13, no. 22, pp. 678–680, Oct. 1977.

[3] K. Jackson, S. Newton, B. Moslehi, M. Tur, C. Cutler, J. Goodman, and H. J. Shaw, "Optical fiber delay-line signal processing," *IEEE Trans. Microw. Theory Tech.*, vol. MTT-33, no. 3, pp. 193–204, Mar. 1985.

[4] D. Davies and G. W. James, "Fiber and integrated optical devices for signal processing," *Electron. Lett.*, vol. 20, no. 2, pp. 95–97, 1984.

[5] R. A. Minasian, K. E. Alameh, and E. H. W. Chan, "Photonics-based interference mitigation filters," *IEEE Trans. Microw. Theory Tech.,* vol. 49, no. 10, pp. 1894–1899, Oct. 2001.
[6] D. Pastor, B. Ortega, P. Y. Fonjallaz, and M. Popov, "Tunable microwave photonic filter for noise and interference suppression in UMTS base stations," *Electron. Lett.*, vol. 40, no. 16, pp. 997–999, Aug. 5, 2004.
[7] G. A. Ball, W. H. Glenn, and W. W. Morey, "Programmable fiber-optic delay line," *IEEE Photon. Technol. Lett.*, vol. 6, no. 6, pp. 741–743, Jun. 1994.
[8] D. B. Hunter and R. A. Minasian, "Photonic signal processing of microwave signals using active-fiber Bragg-grating-pair structure," *IEEE Trans. Microw. Theory Tech.*, vol. 45, no. 8, pp. 1463–1466, Aug. 1997.
[9] J. Mora, B. Ortega, M. V. Andrés, J. Capmany, J. L. Cruz, D. Pastor, and S. Sales, "Tunable all-optical negative multi-tap microwave filters based on uniform fiber Bragg gratings," *Opt. Lett.*, vol. 428, no. 15, pp. 1308–1310, Aug. 2003.
[10] J. Capmany, D. Pastor, A. Martinez, B. Ortega, and S. Sales, "Microwave photonic filters with negative coefficients based on phase inversion in an electro-optic modulator," *Opt. Lett.*, vol. 28, no. 16, pp. 1415–1417, Aug. 2003.
[11] D. B. Hunter, "Incoherent bipolar tap microwave photonic filter based on a balanced bridge electro-optic modulator," *Electron. Lett.*, vol. 40, no. 14, pp. 856–857, Jul. 2004.
[12] D. Pastor, J. Capmany, and B. Ortega, "Reconfigurable RF-photonic filter with negative coefficients and flat top resonances using phase inversion in a newly designed 2×1 integrated Mach–Zehnder modulator," *IEEE Photon. Technol. Lett.*, vol. 16, no. 9, pp. 2126–2128, Sep. 2004.
[13] S. Mansoori, A. Mitchell, and K. Ghorbani, "Photonic reconfigurable microwave filter with negative coefficients," *Electron. Lett.*, vol. 40, no. 9, pp. 541–542, Apr. 2004.
[14] J. Capmany, B. Ortega, D. Pastor, and S. Sales, "Microwave photonic filters using low-cost sources featuring tunability, reconfigurability and negative coefficients," *Opt. Express*, vol. 13, no. 5, pp. 1412–1417, Mar. 2005.
[15] M. Popov, P. Fonjallaz, and O. Gunnarsson, "Compact microwave photonic transversal filter with 40-dB sidelobe suppression," *IEEE Photon. Technol. Lett.*, vol. 17, no. 3, pp. 663–665, Mar. 2005.
[16] *An Introduction to Ultra Wideband Communication Systems*, J. H. Reed, Ed. Upper Saddle River, NJ: Prentice-Hall, 2005.
[17] K. Sasayama, M. Okuno, and K. Habara, "Coherent optical transversal filter using silica-based waveguides for high speed signal processing," *J. Lightw. Technol.*, vol. 9, no. 10, pp. 1225–1230, Sep. 1991.
[18] A. M. Weiner, "Femtosecond pulse shaping using spatial light modulators," *Rev. Sci. Instrum.*, vol. 71, no. 5, pp. 1929–1960, 2000.
[19] M. Shirasaki, "Large angular dispersion by a virtually imaged phased array and its application to a wavelength demultiplexer," *Opt. Lett.*, vol. 21, no. 5, pp. 366–368, 1996.
[20] S. Xiao and A. M. Weiner, "An eight-channel hyperfine wavelength demultiplexer using a Virtually-Imaged Phased-Array (VIPA)," *IEEE Photon. Technol. Lett.*, vol. 17, no. 2, pp. 372–374, Feb. 2005.
[21] ——, "Optical Carrier Suppressed Single Sideband (O-CS-SSB) modulation using a hyperfine blocking filter based on a Virtually-Imaged Phased-Array (VIPA)," *IEEE Photon. Technol. Lett.*, vol. 17, no. 7, pp. 1522–1524, Jul. 2005.
[22] ——, "4-user, $\sim$ 3GHz-spaced Sub-Carrier Multiplexing (SCM) using optical direct-detection via hyperfine WDM," *IEEE Photon. Technol. Lett.*, vol. 17, no. 10, pp. 2218–2220, Oct. 2005.
[23] S. Etemad, P. Toliver, R. Menendez, J. Young, T. Banwell, S. Galli, J. Jackel, P. Delfyett, C. Price, and T. Turpin, "Spectrally efficient optical CDMA using coherent phase-frequency coding," *IEEE Photon. Technol. Lett.*, vol. 17, no. 4, pp. 929–931, Apr. 2005.
[24] G. Lee and A. M. Weiner, "Programmable optical pulse burst manipulation using a Virtually Imaged Phased Array (VIPA) based Fourier transform pulse shaper," *J. Lightw. Technol.*, vol. 23, no. 11, pp. 3916–3923, Nov. 2005.
[25] S. Xiao, A. M. Weiner, and C. Lin, "A dispersion law for virtually-imaged phased array based on paraxial wave theory," *IEEE J. Quantum Electron.*, vol. 40, no. 4, pp. 420–426, Apr. 2004.

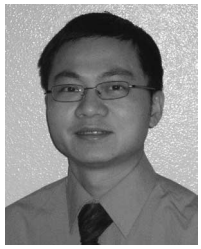

Shijun Xiao (S'03–M'05) was born in Chengdu, China, in 1979. He received the B.S. degree in electronics from Beijing University, Beijing, China, in 2001 and the M.S. and Ph.D. degrees in electrical and computer engineering from Purdue University, West Lafayette, IN, in 2003 and 2005, respectively.

He is currently a Postdoctoral Research Associate with the School of Electrical and Computer Engineering, Purdue University. He was the author or coauthor of nearly 30 journal articles and conference papers. His research interests include optical signal processing, optical pulse shaping, optical fiber communications, microwave photonics, and silicon photonics. His effort has been focused on virtually imaged phased array and its novel applications in optical signal processing and optical fiber communication with a sub-gigahertz channel resolution.

Dr. Xiao is a member of the IEEE Lasers and Electro-Optics Society (LEOS) and the Optical Society of America. He received the Andrews Fellowship from Purdue University from 2001 to 2003, and the IEEE LEOS Graduate Student Fellowship in 2004. He was a Finalist for the Dimitris N. Chorafas Foundation Award of Purdue University in recognition of top Ph.D. research in 2005.

Andrew M. Weiner (S'84–M'84–SM'91–F'95) received the Sc.D. degree in electrical engineering from the Massachusetts Institute of Technology (MIT), Cambridge, in 1984.

From 1979 through 1984, he was a Fannie and John Hertz Foundation Graduate Fellow at MIT. Upon graduation, he joined Bellcore, first as member of Technical Staff and later as Manager of Ultrafast Optics and Optical Signal Processing Research. In 1992, he moved to Purdue University, West Lafayette, IN, and is currently the Scifres Distinguished Professor of Electrical and Computer Engineering (ECE). From 1997 to 2003, he served as ECE Director of Graduate Admissions. His research focuses on ultrafast optical signal processing and high-speed optical communications. He is especially well known for pioneering the field of femtosecond pulse shaping, which enables generation of nearly arbitrary ultrafast optical waveforms according to user specifications. He has published five book chapters and over 160 journal articles and is coeditor of one book. He has been author or coauthor of over 300 conference papers, including approximately 80 conference invited talks, and has presented over 70 additional invited seminars at university, industry, and government organizations. He is holder of eight U.S. patents.

Prof. Weiner has received numerous awards for his research, including the Hertz Foundation Doctoral Thesis Prize in 1984, the Adolph Lomb Medal of the Optical Society of America (OSA) in 1990, awarded for pioneering contributions to the field of optics made before the age of 30, the Curtis McGraw Research Award of the American Society of Engineering Education in 1997, the International Commission on Optics (ICO) Prize in 1997, the IEEE Lasers and Electro-Optics Society (LEOS) William Streifer Scientific Achievement Award in 1999, the Alexander von Humboldt Foundation Research Award for Senior U.S. Scientists in 2000, and the inaugural Research Excellence Award from the Schools of Engineering at Purdue in 2003. He is a Fellow of the OSA. He has served on or chaired numerous research review panels, professional society award committees, and conference program committees. In 1988–1989, he served as an IEEE LEOS Distinguished Lecturer. He has served as Chair or Cochair of the Conference on Lasers and Electro-optics, the Gordon Conference on Nonlinear Optics and Lasers, and the International Conference on Ultrafast Phenomena. He has also served as Associate Editor for IEEE JOURNAL OF QUANTUM ELECTRONICS, IEEE PHOTONICS TECHNOLOGY LETTERS, and *Optics Letters*. From 1997–1999, he served as an elected member of the Board of Governors of IEEE LEOS and as Secretary/Treasurer of IEEE LEOS from 2000–2002. From 2002–2005, he was a Vice-President (representing IEEE LEOS) of the ICO.